PAPR Reduction for Bandwidth-Aggregated OFDM and SC-FDMA Systems

Pochun Yen, Hlaing Minn
University of Texas at Dallas
Richardson, TX 75083 USA
pxy062000@utdallas.edu, hlaing.minn@utdallas.edu

Chia-Chin Chong
DOCOMO Communications Laboratories USA, Inc.
3240 Hillview Avenue, Palo Alto, CA 94304 USA
cchong@docomolabs-usa.com

***Abstract*—Next generation wireless systems require much higher data rate supports and hence larger bandwidths than the existing systems. Due to the compatibility requirement with the existing legacy systems and the constraints on the availability of contiguous spectrum, bandwidth (or carrier) aggregation has recently emerged as a practical means for supporting high data rate requirement of next-generation systems. A practical issue associated with the bandwidth or carrier aggregation is the significant increase of the peak-to-average power ratio (PAPR) of the time-domain signal. This paper proposes a low-complexity PAPR reduction method for bandwidth aggregated systems with orthogonal frequency division multiplexing / multiple-access (OFDM/OFDMA) or single-carrier frequency division multiple access (SC-FDMA). The proposed approach adopts the existing selective mapping concept, but with some modifications for substantially reducing complexity and signaling overhead, while adapting to carrier-aggregated systems. Performance evaluation under 3GPP LTE-Advanced environment shows PAPR reduction advantage of the proposed method while not requiring any signaling overhead.**

***Index Terms*—Carrier aggregation, LTE-Advanced, PAPR, OFDMA, SC-FDMA.**

I. Introduction

Several current and future-envisioned wireless services and applications have motivated the need to support much higher data rate than current systems can provide. The next generation IMT-Advanced system [2] specifies a support of 1 Gbps for environments with low mobility. To meet the data rate requirement of the IMT-Advanced systems, the 3GPP LTE-Advanced (LTE-A) standard plans to use a maximum of 100 MHz bandwidth. On the other hand, due to the compatibility with the existing systems, i.e., LTE Release 8, and the difficulties in obtaining contiguous spectral chunk of 100 MHz, the LTE-A has adopted bandwidth (or carrier) aggregation where several LTE Release 8 component carriers (CCs), which could be non-contiguous in spectral domain, are aggregated in order to provide the targeted data rate. A consequence of the carrier aggregation (CA) is the increase of the peak-to-average power ratio (PAPR) of the time domain signal. Signal with large PAPR will experience nonlinear distortions at the transmit power amplifier, resulting in in-band distortion and out-of-band spectral leakage, which cause performance degradation, interference to other systems, energy inefficiency, reduced cell coverage, and system capacity loss. Hence, PAPR control is an important practical issue for carrier aggregated systems.

There exist several PAPR reduction techniques for orthogonal frequency division multiplexing (OFDM) systems in the literature (see [3] for an overview). One simplistic solution to PAPR problem is to use a transmit power amplifier with a sufficiently large linearity range and an appropriate back-off of the operating point. However, such an approach is highly energy-inefficient and costly, and hence inappropriate for mobile devices. Another way to combat this issue is by clipping and filtering [4]–[6], but it causes undesired out-of-band spectral leakage and performance degradation. Proper designs of pulse shaping filters [10]–[12] can alleviate the PAPR issue but not at a significant level. Several other schemes exploited some system resources (signaling overhead, code rate loss, etc.) to gain substantial PAPR reduction. These schemes include partial transmit sequences (PTS) [7], [8], selective mapping technique (SLM) [15]–[18], block coding [13], [14] and tone reversion [19], [20].

However, all of those works consider typical OFDM systems which are not carrier-aggregated systems. It is unclear that what PAPR reduction techniques will be suitable for the carrier aggregated systems and up to what level of PAPR reduction they can provide. In addition, carrier aggregated systems may employ single carrier frequency division multiple access (SC-FDMA) (as adopted in the uplink (UL) of LTE Release 8 and LTE-A) which has different PAPR characteristics than the OFDM or OFDMA systems [21]. The promising schemes with significant PAPR reduction such as partial transmit sequences and selective mapping technique require substantial signaling overhead. The overhead requirement of such schemes in the CA systems would be increased according to the number of CCs, and the complexity increase would be exponential. These aspects deter their practical applicability to CA systems, especially for mobile devices.

In this paper, we address PAPR reduction of carrier-aggregated OFDM/OFDMA and SC-FDMA systems. While adopting SLM concept, our contributions include (i) the concept of multi-symbol PAPR optimization intervals for signaling overhead reduction, (ii) the exploitation of existing reference symbols for signaling overhead reduction, (iii) the concept of partial group selection for complexity reduction, and (iv) adaptation to CA systems. In particular, we propose a method named partial SLM (PSLM), which provides low-complexity PAPR reduction while requiring no signaling over-

978-1-61284-254-7/11/$26.00 ©2011 IEEE

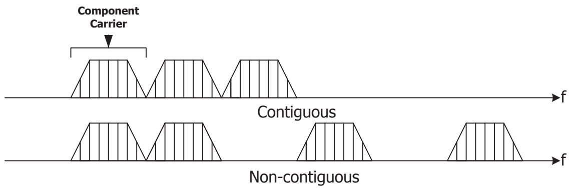

Fig. 1. Contiguous and non-contiguous carrier aggregation of multiple CCs.

head under LTE-A environments. PSLM also offers tradeoff between PAPR reduction and signaling overhead through the adjustment of optimization interval.

The rest of the paper is organized as follows. Section II presents system model, and Section III describes the proposed PSLM method. Simulations results are discussed in Section IV, and Section V concludes this paper.

II. System Model

In this paper, the LTE system is used as the system model[1]. In LTE, OFDMA is adopted in downlink (DL) and SC-FDMA (or discrete Fourier transform (DFT) spread OFDM) is used in UL. The aggregation of several LTE CCs is introduced in the LTE-A standardization process in order to utilize wider bandwidth (for higher data rate) while keeping backward compatibility with the LTE Release 8 standard. Two possible configurations are considered – contiguous and non-contiguous aggregations which are shown in Fig. 1. Each DL/UL transmission subframe for a user on a CC contains several subcarriers over multiple symbols forming a resource grid (RG). We ignore cyclic prefix (CP) in the PAPR calculation since it is merely the cyclic extension of the signal itself.

Let $N_{\rm sc}$ and $N_{\rm symb}$ denote the total number of available subcarriers in each CC and the number of OFDM or SC-FDMA symbols in each subframe, respectively. Define $f_i = f_{c_i} - f_{c_0}$ which represents the center frequency difference of the ith CC and the reference 0th CC in the considered link (DL or UL).

A. DL Model

Denote $\{X_{i,l,k} : \ k \in \boldsymbol{F}_{i,\rm DL}\}$ to be the QAM symbols (or reference tones) at the lth OFDMA symbol of the ith CC, where k is the subcarrier index and $\boldsymbol{F}_{i,\rm DL}$ is the set of the indices of those $N_{\rm sc}$ active subcarriers in the ith CC. $X_{i,l,k}$ is allocated to the (k, l) element of the resource grid. Then, the continuous time baseband signal $s^{\rm DL}_{i,l}(t)$ in the lth OFDMA symbol of the ith CC in a subframe is given by

$$s^{\rm DL}_{i,l}(t) = \sum_{k\in \boldsymbol{F}_{i,\rm DL}} X_{i,l,k} \cdot e^{j2\pi k\Delta f t} e^{j2\pi f_i t}, \qquad (1)$$

for $0 \leq t \leq NT_s$ (which will be shifted to the lth symbol interval later) and $l = 0, \cdots, N_{\rm symb} - 1$, where N is the inverse DFT (IDFT) size without oversampling and T_s is the sample duration. We assume in our PAPR evaluation that all available subcarriers are scheduled to multiple users, hence the system is operating at its maximal capacity.

[1]The proposed scheme can be applied to other OFDM based systems as well.

B. UL Model

Consider that an UL user is assigned with R subcarriers per symbol over $N_{\rm symb}$ SC-FDMA symbols on a CC. Obviously, $R \leq N_{\rm sc}$. Let $\boldsymbol{F}_{i,\rm UL}$ denote the subcarrier index set of the considered UL user on the ith CC. The QAM data (or reference) symbols of the user for the lth SC-FDMA symbol on the ith CC are given as $\{x_{i,l,k}, k = 0, \cdots, R-1\}$. Unlike the DL OFDM scheme, a DFT precoding shall be applied to the QAM data $\{x_{i,l,k}\}$ as

$$X_{i,l,k} = \frac{1}{R}\sum_{m=0}^{R-1} x_{i,l,k} e^{-j\frac{2\pi mk}{R}},\ k = 0, \cdots, R-1, \qquad (2)$$

where l ranges from 0 to $N_{\rm symb} - 1$ except those for the reference signals. The continuous-time baseband signal $s^{\rm UL}_{i,l}(t)$ of the lth SC-FDMA symbol (or reference signal) on the ith CC in an UL time slot is given by

$$s^{\rm UL}_{i,l}(t) = \sum_{k\in \boldsymbol{F}_{i,\rm UL}} X_{i,l,k} \cdot e^{j2\pi k\Delta f t} e^{j2\pi f_i t},\ 0 \leq t \leq NT_s. \qquad (3)$$

III. Proposed PAPR Reduction Scheme

We aim at developing a PAPR reduction scheme which requires relatively low complexity and little or no associated control signaling in CA systems. We adopt the SLM concept originally proposed in [15], but modify it as follows:

- Instead of optimizing PAPR over each OFDM symbol as in the original SLM which requires substantial control signaling overhead, we minimize PAPR defined over several OFDM or SC-FDMA symbols in order to remove (or substantially relieve) the control signaling overhead. Thus, the first step in developing the proposed PAPR reduction scheme is to determine appropriate PAPR optimization intervals.
- In the SLM, all subcarrier data of each OFDM symbol are divided into several disjoint groups and phase rotations are applied group-wise (the same phase within each group) across all groups in minimizing the PAPR. In contrast, to reduce the complexity, we apply phase rotations to only a subset of the SLM groups (thus, we call it partial SLM (PSLM) afterwards, see Fig. 3). For modularity across CCs, we adopt the same subset of the SLM groups for all CCs. Hence, the second step is to determine the total number of groups and the number of selected groups, as well as how to select them.
- The PAPR is now defined as that of the CA signal consisting of several CCs which pass through the same RF chain.
- The PAPR optimization is performed jointly across all related CCs.

A. PAPR Optimization Interval

The choice of the PAPR optimization interval (the number of OFDM/SC-FDMA symbols over which PAPR is defined and minimized) is constrained by the tradeoff between PAPR

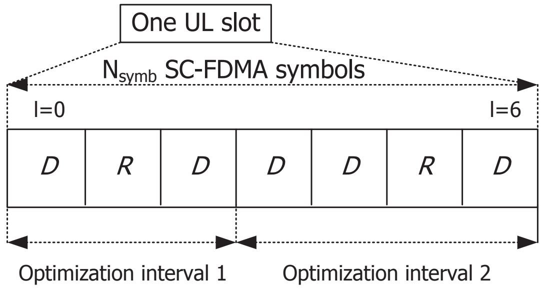

Fig. 2. One UL SC-FDMA time slot where D and R refer to data and reference symbol, respectively.

reduction capability and control signaling overhead. The optimization interval of one symbol provides the best PAPR reduction capability at the cost of substantial control signaling overhead. On the other hand, using the interval with a very large number of symbols will substantially save the signaling overhead but the PAPR reduction might be negligible or unjustifiable for the associated complexity. Thus, a proper tradeoff is necessary. Based on our investigation, we recommend a PAPR optimization interval of around four symbols for SC-FDMA based systems while for OFDM DL systems, a larger interval may be selected which still provides substantial PAPR reduction.

As pilots or reference symbols are typically transmitted in practical systems, we can take advantage of them in removing or reducing the control signaling overhead. By including reference symbols in the optimization interval, i.e., applying the same phase rotations for both reference symbols and data symbols, the effects of the phase rotations can be absorbed in the channel estimates. By this way, no separate signaling overhead is required to inform the receiver of the applied phase rotations.

A transmission frame may contain more than one reference symbols. In this case, we may have more than one PAPR optimization intervals. To illustrate, let us consider the UL of the LTE-A system. There are $N_{\text{symb}} = 7$ symbols (normal CP length) in a slot and reference symbols for UL are placed at either third, fourth and fifth SC-FDMA symbols or at second and sixth SC-FDMA symbols. Considering the latter, we can form two PAPR optimization intervals of three symbols and four symbols, with the corresponding symbol index sets $\mathcal{T}_1 = \{0, 1, 2\}$ and $\mathcal{T}_2 = \{3, 4, 5, 6\}$, in each slot as shown in Fig. 2. As there is one reference symbol in each interval, we do not need any control signaling overhead at all in this case.

For an arbitrary system which transmits only one reference symbol in every slot of N_{symb} symbols, we can divide the whole N_{symb} symbols into intervals of four or three symbols for SC-FDMA systems (could choose larger intervals for OFDMA DL) for PAPR optimization. In this case, except for the interval which contains the reference symbol, control signaling is required for all other intervals to inform the receiver of the phase rotations. These control information may be transmitted in the interval with the reference symbol, and for this purpose, the PAPR optimization of the other intervals should be done first.

B. Group Selection

The total number of groups denoted by S as well as the number of selected groups denoted by K provide a tradeoff between PAPR reduction capability and complexity (plus overhead). The underlying system parameters (e.g., resource block sizes) also shape the choice of those group numbers. In LTE-A UL environments, with the consideration of low complexity, a good choice is $S = 6$ total groups and $K = 3$ selected groups.

The other aspect that should be considered is how to address for different resource block sizes especially for UL. In order to limit the complexity regardless of the resource block size, we adopt to use a fixed number of groups while adjusting the size of each group to accommodate for the change in the resource block size.

The next step is to find out which groups should be selected. For example, in the above mentioned LTE-A scenario with three selected groups out of six groups, there are 20 possible selections and it is unlikely that all will give the same PAPR reduction performance. As our results will show later in this paper, a proper selection does yield a better PAPR reduction performance.

As DL contains data for all users, it has much larger resource size than the UL. The same procedure can be applied for DL but the values of S and K can be chosen differently (especially, larger than UL case to gain more PAPR reduction) if desired. On the other hand, base stations typically have power amplifiers with large linearity range and energy consumption is not a concern. Hence, even using the same values of S and K as in the UL may be sufficient for the DL.

Note that all the steps in this subsection can be done offline once, and hence there is no implementation complexity associated with this group selection. The group numbers and selection are fixed across all CCs. This provides simplicity and modularity in implementation.

C. PAPR Reduction

Consider a PAPR optimization interval denoted by the symbol index set $\mathcal{T}$. From (1) and (3), we can write the carrier-aggregated continuous-time signal $s_{\text{CA}}(t)$ over the above interval as

$$s_{\text{CA}}(t) = \sum_{l \in \mathcal{T}} \sum_{i=0}^{M-1} s_{i,l}(t - lNT_s) \cdot g(t - lNT_s), \quad (4)$$

where $s_{i,l}(t)$ is either the baseband OFDM signal $s_{l,i}^{\text{DL}}(t)$ or SC-FDMA signal $s_{i,l}^{\text{UL}}(t)$ in ith CC, M is the number of CCs transmitted through the same RF chain and $g(t)$ is the time-domain windowing function for which we adopt a rectangular function.

PSLM starts with dividing the RG of each CC over the above optimization interval, for either OFDM or SC-FDMA system, into S groups of subcarriers. In other words, all symbols which form a vector $\mathbf{X}_{i,l,k}$ of the IDFT input in

ith CC are partitioned into S disjoint sets, represented by $\{\mathbf{X}_{i,l}^{(q)}, q = 0, \cdots, S-1\}$. Therefore, the $s_{\mathrm{CA}}(t)$ in (4) before applying phase rotation can be rewritten as

$$\begin{aligned} s_{\mathrm{CA}}(t) &= \sum_{l\in\mathcal{T}} \sum_{i=0}^{M-1} s_{i,l}(t - lNT_s) g(t - lNT_s) \\ &= \sum_{l\in\mathcal{T}} \sum_{i=0}^{M-1} \sum_{k\in\boldsymbol{F}_i} X_{i,l,k} e^{j2\pi(k\Delta f + f_i)(t-lNT_s)} g(t - lNT_s) \\ &= \sum_{l\in\mathcal{T}} \sum_{i=0}^{M-1} \sum_{q=0}^{S-1} \sum_{k\in\mathbf{J}_{i,l,q}} \\ &\quad \mathbf{X}_{i,l,k} e^{j2\pi(k\Delta f + f_i)(t-lNT_s)} g(t - lNT_s), \end{aligned} \tag{5}$$

where the set $\mathbf{J}_{i,l,q}$ contains indices of all subcarriers which belong to the qth group and $\boldsymbol{F}_i$ is either $\boldsymbol{F}_{i,\mathrm{DL}}$ in (1) or $\boldsymbol{F}_{i,\mathrm{UL}}$ in (3).

Next, PSLM applies phase rotations to the selected groups. The phase rotation $\phi_{i,q}$ which rotates the ith CC's qth group is from the set $\boldsymbol{\Phi} = \{\Phi_p : p = 0, \cdots, P-1\}$, where P is the number of phase choices applied to each group of subcarriers. Therefore, the partially phase shifted signal corresponding to a phase combination $\mathbf{v}$, denoted by $\tilde{s}_{\mathrm{CA}}(\mathbf{v}, t)$, can be represented as

$$\begin{aligned} \tilde{s}_{\mathrm{CA}}(\mathbf{v}, t) = &\sum_{l\in\mathcal{T}} \sum_{i=0}^{M-1} \sum_{q=0}^{S-1} \sum_{k\in\mathbf{J}_{i,l,q}} \\ &\mathbf{X}_{i,l,k} e^{j\phi_{i,q}} e^{j2\pi(k\Delta f + f_i)(t-lNT_s)} g(t - lNT_s), \end{aligned} \tag{6}$$

where vector $\mathbf{v} \in \boldsymbol{\Phi}^{KM}$ represents a combination of phases applied. One of the combinations, in particular, is all zeros. Note that the phases $\{\phi_{i,q}\}$ of the unselected groups are set to zero. Each group of subcarriers in one CC has P applicable different phases, K selected groups are in one CC and there are M CCs in total. Hence, P^{KM} combinations of phase rotations are available to apply to the RGs differently. Each combination results in a different final PAPR value. The transmitter will simply choose the combination which results in the minimal PAPR value. Denote $\mathbf{V}$ as the collection of all possible combinations of phases and each vector $\mathbf{v}$ inside represents one possible phase combination. Therefore, we can write the time-domain transmit signal which has the minimum PAPR as

$$s^*_{\mathrm{CA}}(t) = \tilde{s}_{\mathrm{CA}}(\mathbf{v}^*, t), \tag{7}$$

where

$$\mathbf{v}^* = \arg\min_{\mathbf{v}\in\mathbf{V}} \mathrm{PAPR}\left[\tilde{s}_{\mathrm{CA}}(\mathbf{v}, t)\right], \tag{8}$$

and

$$\mathrm{PAPR}\left[\tilde{s}_{\mathrm{CA}}(\mathbf{v}, t)\right] = \frac{\max \|\tilde{s}_{\mathrm{CA}}(\mathbf{v}, t)\|^2}{\mathrm{E}\left[\|\tilde{s}_{\mathrm{CA}}(\mathbf{v}, t)\|^2\right]}. \tag{9}$$

The time interval over which the above PAPR is computed is defined by the PAPR optimization interval. Note that when there is a reference symbol within the optimization interval, the PAPR minimized signal can be easily demodulated and decoded at the receiver without the need of extra signaling. As the same phase rotations are applied for reference and data symbols within an optimization interval, the effects of phase rotations are compensated by the channel equalization process automatically.

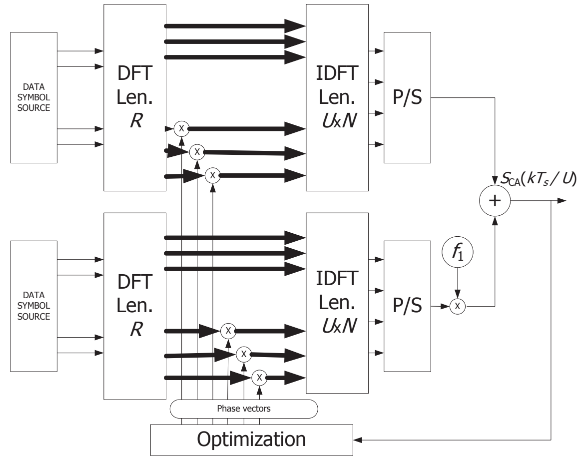

Fig. 3. Block diagram of the proposed method in UL scenario with 2 CCs. PAPR optimization is typically done in all discrete-time domain and in this case a larger IDFT size (where U is the oversampling factor) should be used.

IV. Performance Evaluation

A. Simulation Parameters

System parameters are adopted from the current LTE-A specification up to date [2]. Although the standardization of LTE-A is still under way, most of the ongoing activities focus on higher layer formatting and protocols, and the physical layer aspects related to PAPR are already fixed, e.g. $N_{\mathrm{sc}} = 1320$ and $\Delta f = 15$kHz. The oversampling factor for PAPR calculation is $U = 8$, and hence IDFT size of each CC is $N \times U = 2048 \times 8 = 16384$ for the reliable computation of PAPR. The predefined phases set is $\Phi = \{0, \pi\}$. To evaluate CA systems without complexity burden, we use two non-contiguous CCs for the UL and three contiguous or non-contiguous CCs for the DL in our simulation. We expect that the use of larger number of CCs would give larger PAPR reduction.

For the UL where SC-FDMA is used, $N_{\mathrm{symb}} = 7$ symbols per time slot is used and the PAPR optimization intervals within a time slot are set as shown in Fig. 2. The considered UL user occupies $R = 72$ subcarriers (contiguous) over all $N_{\mathrm{symb}} = 7$ symbols per time slot on each CC. Each UL CC of a user is divided into $S = 6$ groups and $K = 3$ groups are selected for phase rotation. In DL OFDM scenario, we assume all 1320 subcarriers are occupied by multiple users on each CC. We form $S = 10$ groups in each DL CC and only $K = 3$ groups are phase-rotated. Here, we set a PAPR optimization interval to be the subframe length ($N_{\mathrm{symb}} = 14$ symbols) of the LTE-A frame structure. This setting of large optimization interval is just to illustrate that in DL even with such a large interval, a substantial PAPR reduction can be obtained due to

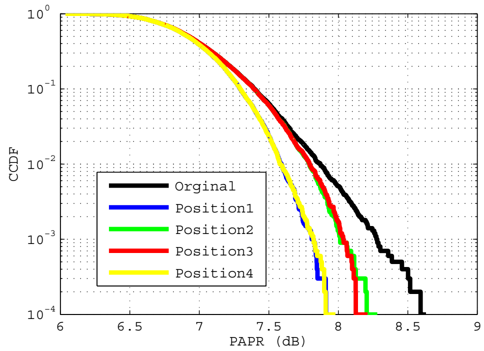

Fig. 4. Effect of group selection in UL SC-FDMA with QPSK modulation, obtained by 10,000 iterations.

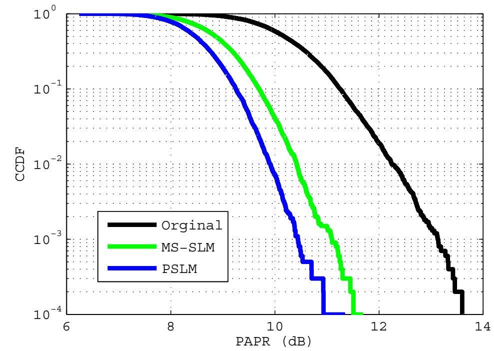

Fig. 5. PAPR characteristics of the proposed schemes with the optimization of 3 symbols in UL SC-FDMA with 16-QAM modulation, obtained by 10,000 iterations.

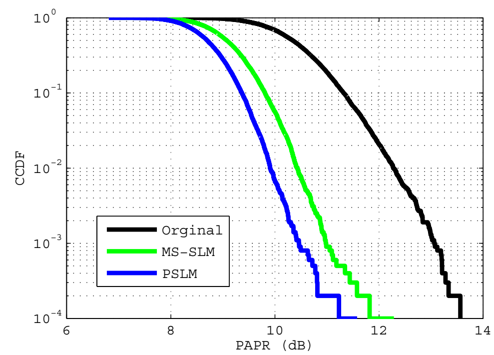

Fig. 6. PAPR characteristics of the proposed schemes with the optimization interval of 4 symbols in UL SC-FDMA, 16-QAM modulation, obtained by 10,000 iterations.

large number of subcarriers involved. In fact, the same two optimization intervals of UL can be applied to the DL LTE-A since there are two reference symbols in each DL slots.

We evaluate two PAPR reduction schemes, the proposed PSLM and the SLM applied over multiple symbols. The latter is named as multi-symbol SLM (MS-SLM) to reflect the multi-symbol PAPR optimization interval, and to maintain the same complexity as in PSLM, we use three total groups per CC, all of which are subject to phase rotations. The SLM scheme which operates on each symbol is not considered in this paper simply due to the large signaling overhead requirement. In the performance comparison, we also include the original CA signal without any modification which is denoted "Original" in the figures.

B. Results and Discussion

First, we evaluate the effect of group selection in LTE-A UL scenario. All 20 possible positions of the three selected groups are evaluated by simulation, and some selected results in terms of the complementary cumulative distribution function (CCDF) of PAPR are shown in Fig. 4. Position 1 curve represents the case where the three phase-rotated groups are located at the last three group locations. Position 2 curve corresponds to the 3rd, 4th and 5th group locations. Position 3 curve selects the 2nd, 3rd and 4th group locations, while Position 4 curve chooses the first three group locations. The results show that the group selection can make a difference in PAPR reduction and Position 1 and 4 have the lowest PAPR results among all possible location placements. Hence, the group selection corresponding to Position 1 is adopted in the rest of the simulations.

The CCDF performances for the UL are shown in Fig. 5 for the optimization interval of three symbols and in Fig. 6 for the four symbols interval (c.f. Fig. 2). The MS-SLM provides about 2.5 dB PAPR reduction over the original signal, while the PSLM achieves about 3 dB PAPR reduction. The additional 0.5 dB gain is due to the partial group selection feature. Considering that SC-FDMA already has relatively lower PAPR than OFDM, these PAPR performance improvements are very promising, especially for mobile devices.

The DL results are shown in Fig. 7 and Fig. 8 for the contiguous CA and non-contiguous CA scenario, respectively. We observe that the PAPR reduction gains (more than 3 or 4 dB) are even larger than those in the UL. Although base stations can handle much larger PAPR than mobile devices, the use of multiple CCs results in relatively large PAPR even for the base stations as can be seen in the figures. This increased PAPR can adversely affect device energy efficiency and cost if the power amplifier is specifically designed to handle it, or performance degradation and out-of-band spectral leakage if the linearity range of the power amplifier is not sufficient to handle it. Furthermore, lowering PAPR at the base station can improve the cell coverage and reduce the cost of deployment.

Next, we discuss the complexity and signaling overhead requirements of different schemes using the LTE-A UL scenario as an example. In our UL simulation scheme, the original SLM [15] requires $M \times N_{\text{symb}} \times P^{SM} = 2 \times 7 \times 2^{6\times 2} = 57,344$ IDFT operations with IDFT size $N \times U = 16,384$, $N_{\text{symb}} \times P^{SM} = 7 \times 2^{6\times 2} = 28672$ PAPR calculations, each based on $16,384$ samples, and $N_{\text{symb}} \times \lceil \log_2 P^{SM} \rceil = 84$ bits for control overhead; hence it is not practically appealing due to its high complexity and overhead. On the other hand, PSLM and MS-SLM only require 896 IDFT operations with IDFT size $16,384$, and 192 PAPR calculations based

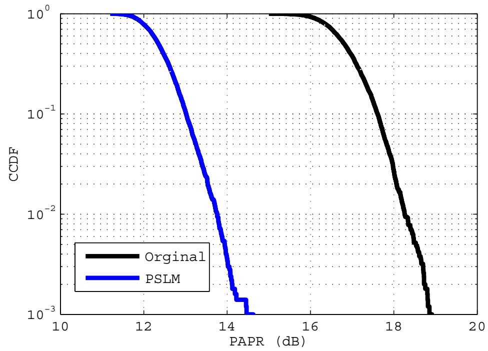

Fig. 7. PAPR characteristics of the proposed schemes in DL OFDM with 3 contiguous CCs and 16-QAM modulation, obtained by 5000 iterations

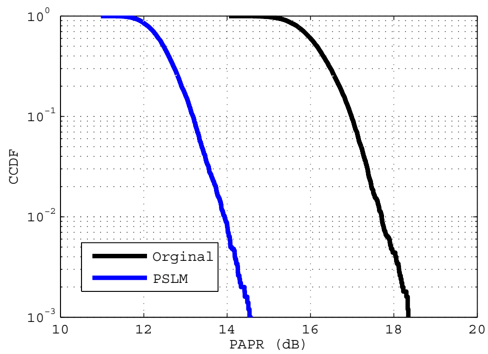

Fig. 8. PAPR characteristics of the proposed schemes in DL OFDM with 3 non-contiguous CCs and 16-QAM modulation, obtained by 5000 iterations

on $16384 \times 3 = 49,152$ samples when using optimization interval of 3 symbols and 256 PAPR calculations based on $16384 \times 4 = 65,536$ samples for 4 symbols, while not needing any control bits related to PAPR reduction.

V. Conclusions

Next generation wireless communication systems utilize wider bandwidth by aggregating many smaller bands (or component carriers); therefore, PAPR becomes an even more severe issue for those systems. We have presented PAPR reduction schemes for carrier-aggregated systems, using OFDMA and SC-FDMA as in the LTE-A standard as an example. As the PAPR problem is a practical issue, complexity and control signaling overhead requirements of the PAPR reduction schemes are also of importance. We have proposed the use of multi-symbol PAPR optimization intervals as well as the existing reference symbols for control overhead reduction, and the partial group selection for complexity reduction while maintaining good PAPR reduction performance. Simulation results under LTE-A UL and DL scenarios corroborate significant PAPR reduction performance of the proposed schemes with low complexity and no signaling overhead. The proposed PSLM method offers a quite appealing solution to the PAPR problem of the carrier-aggregated systems.

References

[1] 3GPP TS 36.211: "Evolved Universal Terrestrial Radio Access (E-UTRA); Physical Channels and Modulation," Release 9, Dec. 2009.

[2] 3GPP TR 36.913: "Requirements for further advancements for Evolved Universal Terrestrial Radio Access (E-UTRA) (LTE-Advanced)," Release 9, Dec. 2009.

[3] S. H. Han and J. H. Lee, "An overview of peak-to-average power ratio reduction techniques for multicarrier transmission," *IEEE Wireless Comm. Mag.,* vol. 12, no. 2, pp. 56-65, Apr. 2005.

[4] X. Li and L. J. Jr. Cimini, "Effects of clipping and filtering on the performance of OFDM," *IEEE Commun. Lett.,* vol. 2, no. 5, pp. 131-133, May. 1998.

[5] L. Wang and C. Tellambura, "A simplified clipping and filtering technique for PAR reduction in OFDM systems," *IEEE Signal Process. Lett.,* vol. 12, no. 6, pp. 453-456, Jun. 2006.

[6] H. Ochiai and H. Imai, "Performance analysis of deliberately clipped OFDM signals," *IEEE Trans. Commun.,* vol. 50, no. 1, pp. 89-101, Jan. 2002.

[7] S. H. Muller and J. B. Huber, "OFDM with reduced peak-to-average power ratio by optimum combination of partial transmit sequences," *IEEE Electronics Lett.,* vol. 33, no. 5, pp. 368-369, Feb. 1997.

[8] S. G. Kang, J. G. Kim and E. K. Joo, "A novel subblock partition scheme for partial transmit sequence OFDM," *IEEE Trans. Broadcast.,* vol. 45, no. 3, pp. 333-338, Sep. 1999.

[9] T. Jiang, W. Xiang, P. C. Richardson, J. Guo and G. Zhu, "PAPR Reduction of OFDM Signals Using Partial Transmit Sequences With Low Computational Complexity," *IEEE Trans. Broadcast.,* vol. 53, no. 3, pp. 719-724, Sep. 2007.

[10] S. B. Slimane, "Peak-to-average power ratio reduction of OFDM signals using pulse shaping", *IEEE GLOBECOM,* pp. 1412-1416 vol. 3, 2000.

[11] M. Tanahashi, H. Ochiai, "On the distribution of instantaneous power in single-carrier signals," *IEEE Trans. Wireless Commun.,* vol. 9, no. 3, pp. 1207-1215, Mar. 2010.

[12] N. J. Baas, D. P. Taylor, "Pulse shaping for wireless communication over time- or frequency-selective channels," *IEEE Trans. Commun.,* vol. 52, no. 9, pp. 1477- 1479, Sep. 2004.

[13] D. Wulich, L. Goldfeld, "Reduction of peak factor in orthogonal multicarrier modulation by amplitude limiting and coding," *IEEE Trans. Commun.,* vol. 47, no. 1, pp. 18-21, Jan. 1999.

[14] C. Ciochina, D. Castelain, D. Mottier and H. Sari, "New PAPR-preserving mapping methods for single-carrier FDMA with space-frequency block codes," *IEEE Trans. Wireless Commun.,* vol. 8, no. 10, pp. 5176-5186, Oct. 2009.

[15] R. W. Bauml, R. F. H. Fischer and J. B. Huber, "Reducing the peak-to-average power ratio of multicarrier modulation by selected mapping," *IEEE Electronics Lett.,* vol. 32, no. 22, pp. 2056-2057, Oct. 1996.

[16] R. J. Baxley and G. T. Zhou, "Comparing Selected Mapping and Partial Transmit Sequence for PAR Reduction," *IEEE Trans. Broadcast,* vol. 53, no. 4, pp. 797-803, Dec. 2007.

[17] E. S. Hassan, S. E. El-Khamy, M. I. Dessouky, S. A. El-Dolil and F. E. Abd El-Samie, "Peak-to-average power ratio reduction in space-time block coded multi-input multi-output orthogonal frequency division multiplexing systems using a small overhead selective mapping scheme," *IET Commun.,* vol. 3, no. 10, pp. 1667-1674, Oct. 2009.

[18] M. S. Baek, M. J. Kim, Y. H. You and H. K. Song, "Semi-blind channel estimation and PAR reduction for MIMO-OFDM system with multiple antennas" *IEEE Trans. Broadcast.,* vol.50, no.4, pp. 414- 424, Dec. 2004

[19] D. W. Lim, H. S. Noh, H. B. Jeon, J. S. No and D. J. Shin, "Multi-Stage TR Scheme for PAPR Reduction in OFDM Signals," *IEEE Trans. Broadcast.,* vol. 55, no. 2, pp. 300-304, Jun. 2009.

[20] J. C. Chen and C. P. Li, "Tone Reservation Using Near-Optimal Peak Reduction Tone Set Selection Algorithm for PAPR Reduction in OFDM Systems," *IEEE Signal Processing Letters,* vol. 17, no. 11, pp. 933-936, Nov. 2010.

[21] H. G. Myung, J. Lim and D. J. Goodman, "Peak-To-Average Power Ratio of Single Carrier FDMA Signals with Pulse Shaping," IEEE PIMRC, pp. 1-5, Sep. 2006.

[22] M. M. Rana, M. S. Islam, A. Z. Kouzani, "Peak to Average Power Ratio Analysis for LTE Systems," ICCSN, pp. 516-520, Feb. 2010.